

## Supporting information

# A lactic acid dioxolane as a bio-based solvent for lithium-ion batteries: physicochemical and electrochemical investigations of lithium imide-based electrolytes

Massimo Melchiorre,<sup>a,b</sup> Khai Shin Teoh,<sup>c,d</sup> Juan Luis Gómez Urbano,<sup>c,d</sup> Francesco Ruffo<sup>\*a,e</sup>, and Andrea Balducci<sup>\*c,d</sup>

<sup>a</sup> Dipartimento di Scienze Chimiche, Università degli Studi di Napoli Federico II, Complesso Universitario di Monte S. Angelo, via Cintia 21, 80126, Napoli, Italy

<sup>b</sup> ISusChem Srl, Piazza Carità, 32, 80134, Napoli, Italy

<sup>c</sup> Institute for Technical Chemistry and Environmental Chemistry, Friedrich-Schiller University Jena. Philosophenweg 7a, 07743 Jena, Germany.

<sup>d</sup> Center for Energy and Environmental Chemistry Jena (CEEC Jena). Friedrich-Schiller University Jena. Philosophenweg 7a, 07743 Jena, Germany.

<sup>e</sup> Consorzio Interuniversitario di Reattività Chimica e Catalisi (CIRCC), Via Celso Ulpiani 27, 70126, Bari, Italy.

E-mail: [ruffo@unina.it](mailto:ruffo@unina.it); [andrea.balducci@uni-jena.de](mailto:andrea.balducci@uni-jena.de)

### Table of Contents

<b>Table S1.</b> Relevant parameters for LA-H,H and benchmark EC, DMC and EC/DMC (1:1 vol) solvents. ....	2
<b>Fig. S1.</b> LA-H,H solvent density over 0-80 °C temperature range. ....	3
<b>Fig. S2.</b> Electrolyte density measured over 10-80 °C temperature range. ....	3
<b>Fig. S3.</b> Electrochemical stability window. Cell set-up: WE, Pt or GC disc; <i>quasi</i> -RE Ag; CE, self-standing active carbon electrode. Potential vs Li <sup>+</sup> /Li was estimated considering the Li vs Ag potential (+3.05 V). ....	4
<b>Fig. S4.</b> Example of potential profile of a) LA-H,H-LiFSI 1M and b) LA-H,H LiTFSI over cycling at 0.05 C and 0.1 C without additive, and c,d) with 2% <sub>wt</sub> of VC with GR. e) First cycle at 0.1 C of LA-H,H-LiFSI 1M 2% <sub>wt</sub> VC, and f) C-rate performance over cycling. C.E.: Coulombic Efficiency. ..	5
<b>Fig. S5.</b> Galvanostatic charge/discharge profile with LAHH-LiFSI 1M VC 5% <sub>wt</sub> of a) 1 <sup>st</sup> cycle at 0.05 C, and b) profiles at different current densities over capability test with GR. C.E.: Coulombic Efficiency. ....	6
<b>Fig. S6.</b> a) Rate capability and b) cyclability of LA-H,H imide-electrolytes with 10 % <sub>wt</sub> of VC with graphite electrodes. C.R.: Capacity Retention. ....	6
<b>Fig. S7.</b> LFP galvanostatic charge/discharge profile with LA-H,H-LiFSI 1M VC 5% <sub>wt</sub> of a) 1 <sup>st</sup> cycle at 0.05 C, and b) profiles at different current densities over capability test. C.E.: Coulombic Efficiency. ....	7
<b>Fig. S8.</b> a) Rate capability and b) cyclability of 1EC:1DMC-LiPF <sub>6</sub> 1M electrolyte (LP30) with LFP electrodes. ....	7
<b>Fig. S9.</b> LFP/graphite LIB full-cell a) galvanostatic charge/discharge profiles with LA-H,H-LiTFSI 1M VC 5%wt for noted current densities, and b) profiles of the full-cell, LFP and graphite electrode at 1 C. ....	8
<b>Fig. S10.</b> Relevant 1H NMR spectra (80-100 mg in 0.5 mL CDCl <sub>3</sub> ) of LA-H,H distillation: a) “head”, and b) core fractions. Asterisks (*) are used to highlight <sup>13</sup> C coupling. LA-H,H purity is evaluated by the ratio of the normalized integrals. In spectrum a) the purity was assessed < 99 % (98.4 %), while in spectrum b) it was assessed > 99 % (99.7 %). ....	9
<b>Paragraph S1.</b> NMR analysis details. ....	10
<b>References.</b> ....	10

**Table S1.** Relevant parameters for LA-H,H and benchmark EC, DMC and EC/DMC (1:1 vol) solvents.

Parameter	EC	DMC	EC:DMC	LA-H,H
Density [g mL <sup>-1</sup> ]	1.32 at 40 °C <sup>1</sup>	1.07 at 25 °C <sup>2</sup>	1.21 at 20 °C <sup>3</sup>	1.12 at 20 °C*
Volumetric expansion [°C <sup>-1</sup> ]	0.0007 <sup>4</sup>	0.0013 <sup>5</sup>	0.0012 <sup>3</sup>	0.0010*
Viscosity [mPa s]	1.9 at 40 °C <sup>6</sup>	0.585 at 25 °C <sup>7</sup>	1.68 at 20 °C <sup>8</sup>	1.73 at 20 °C*
Vapor pressure [mmHg]	0.16 at 20 °C <sup>1</sup>	18 at 21.1°C <sup>2</sup>	n.d.	1.7 at 25 °C <sup>9</sup>
Boiling point [°C]	248 <sup>1</sup>	90 <sup>2</sup>	n.d.	161 – 164 <sup>10</sup>
Melting point [°C]	36 <sup>1</sup>	2-4 <sup>2</sup>	7.9 <sup>11</sup>	< -70 <sup>10</sup>
Flash point [°C]	143 <sup>1</sup>	16 <sup>2</sup>	24 <sup>8</sup>	60*
Dielectric constant	89.8 <sup>12</sup>	3.1 <sup>12</sup>	23 <sup>13</sup>	n.d.
Hazardous potential <sup>#</sup>	High <sup>14</sup>	Low <sup>14</sup>	High <sup>14</sup>	Low <sup>10</sup>

\* This work

<sup>#</sup> Hazardous potential specifics: **EC**, this substance is harmful if swallowed, causes serious eye irritation and may cause damage to organs through prolonged or repeated exposure; **DMC**, this substance is a highly flammable liquid and vapour. **EC:DMC**, as mixture, it was reported in the table with a label of the more hazardous component. **LA-H,H**, this substance is not registered by the European Chemical Agency (REACH regulation), its computational structure-response investigation indicate that this substance might be non-carcinogenic and non-reprotoxic

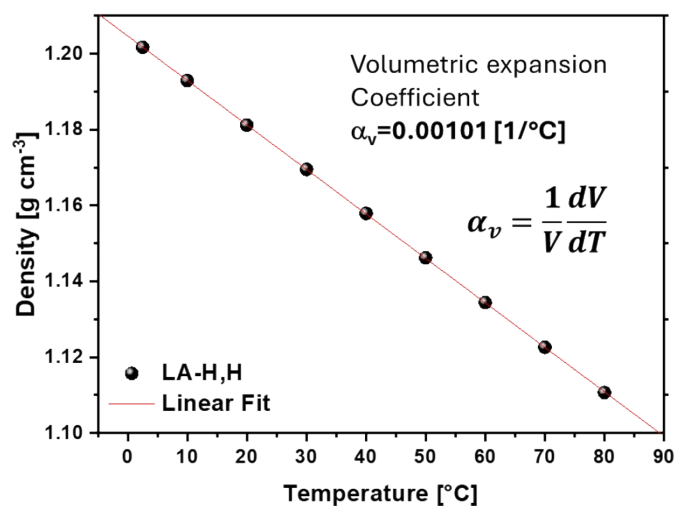


Fig. S1. LA-H,H solvent density over 0-80 °C temperature range.

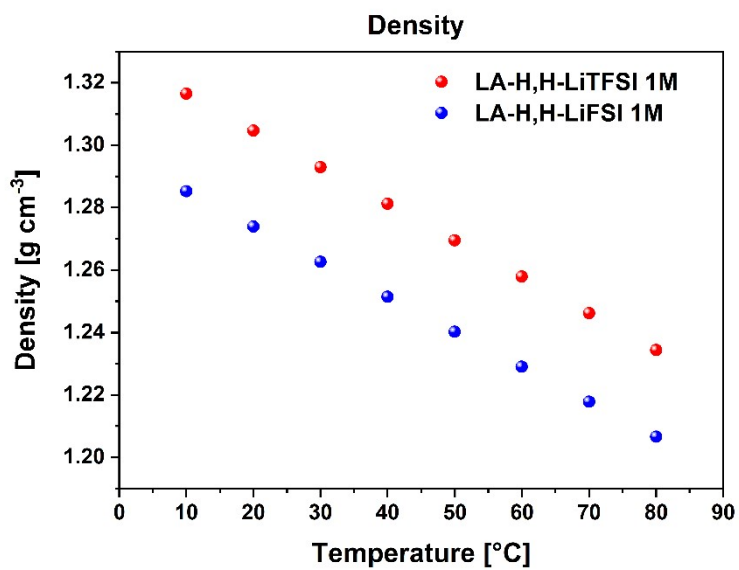
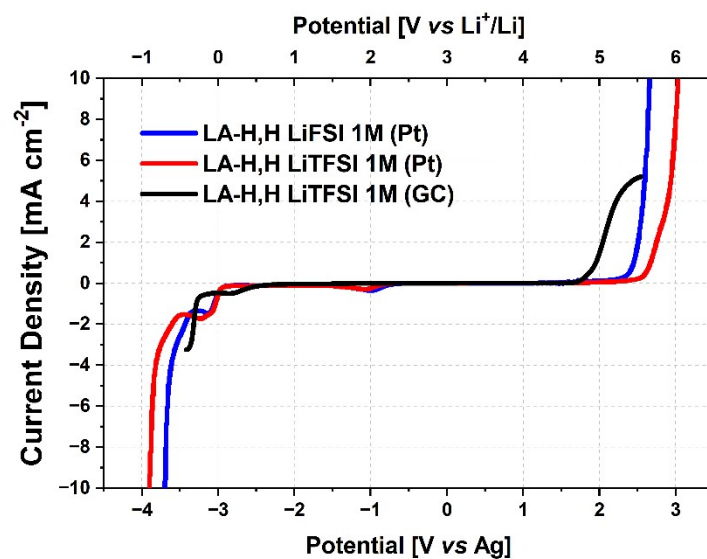
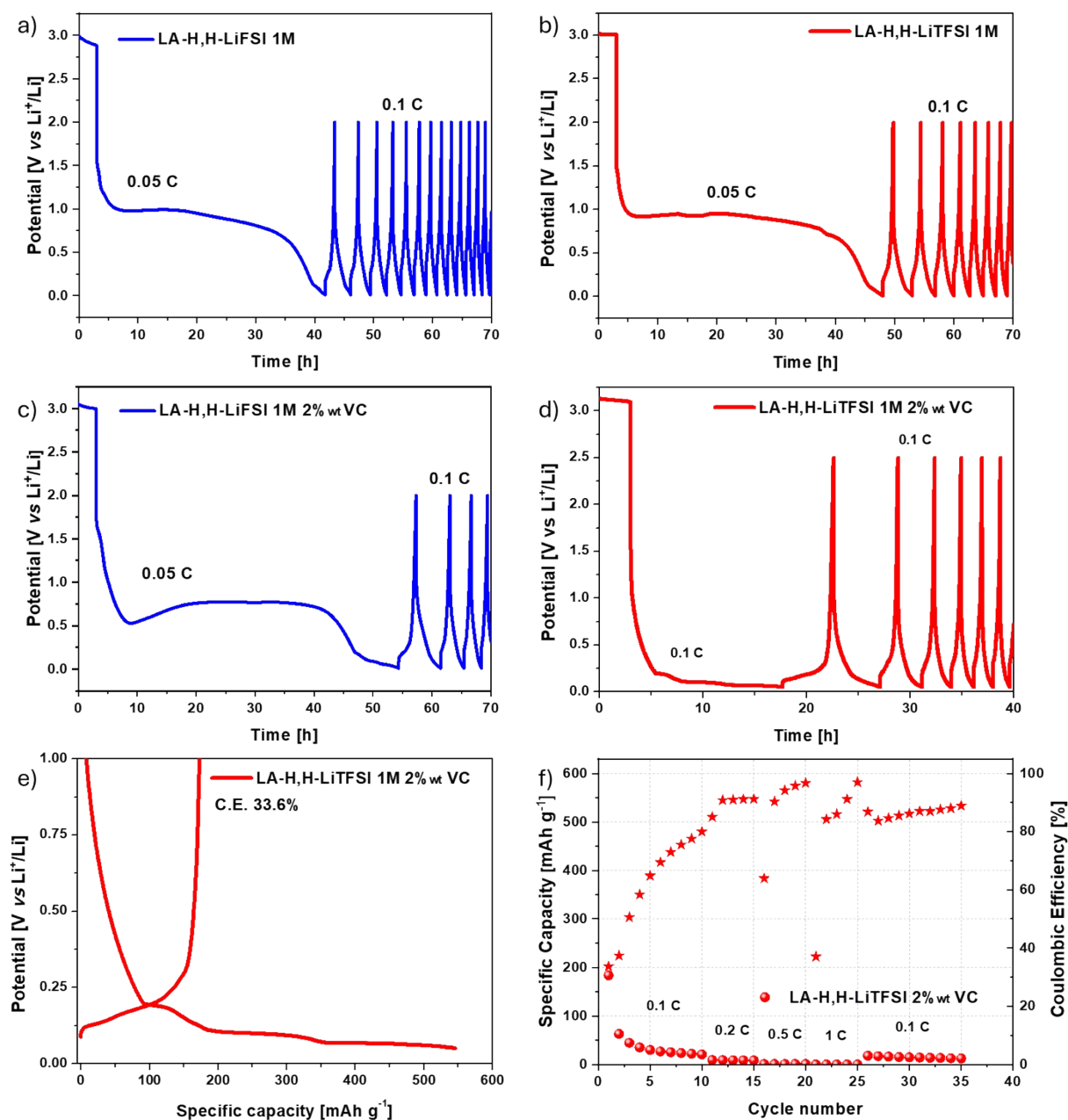


Fig. S2. Electrolyte density measured over 10-80 °C temperature range.



**Fig. S3.** Electrochemical stability window. Cell set-up: WE, Pt or GC disc; *quasi*-RE Ag; CE, self-standing active carbon electrode. Potential vs Li<sup>+</sup>/Li was estimated considering the Li vs Ag potential (+3.05 V).



**Fig. S4.** Example of potential profile of a) LA-H,H-LiFSI 1M and b) LA-H,H-LiTFSI over cycling at 0.05 C and 0.1 C without additive, and c,d) with 2%<sub>wt</sub> of VC with GR. e) First cycle at 0.1 C of LA-H,H-LiTFSI 1M 2%<sub>wt</sub> VC, and f) C-rate performance over cycling. C.E.: Coulombic Efficiency.

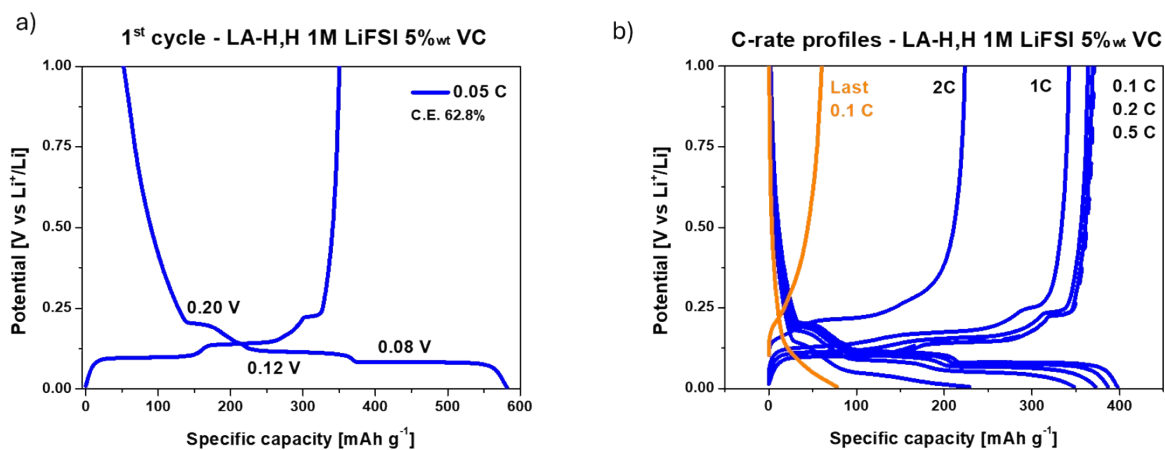


**Fig. S5.** Galvanostatic charge/discharge profile with LAHH-LiFSI 1M VC 5%<sub>wt</sub> of a) 1<sup>st</sup> cycle at 0.05 C, and b) profiles at different current densities over capability test with GR. C.E.: Coulombic Efficiency.

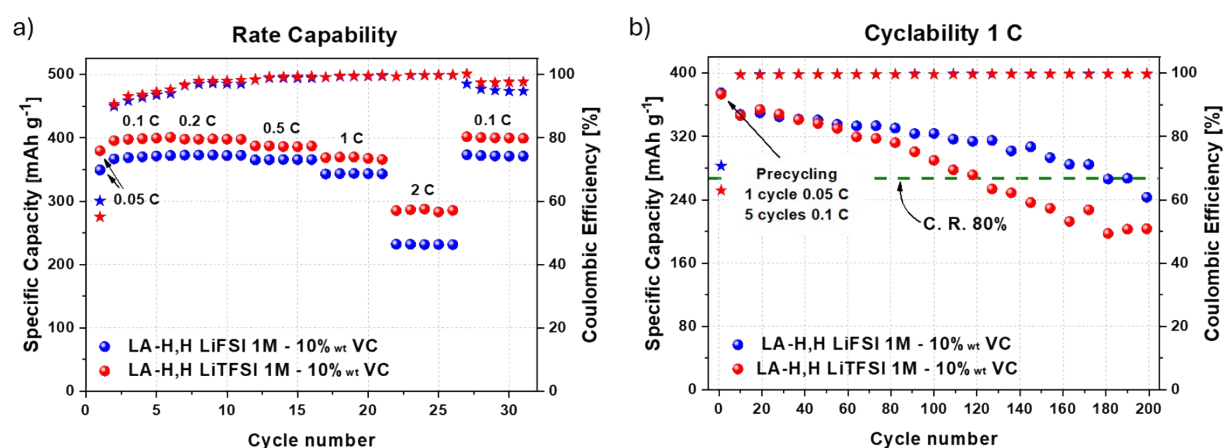


**Fig. S6.** a) Rate capability and b) cyclability of LA-H,H imide-electrolytes with 10 %<sub>wt</sub> of VC with graphite electrodes. C.R.: Capacity Retention.

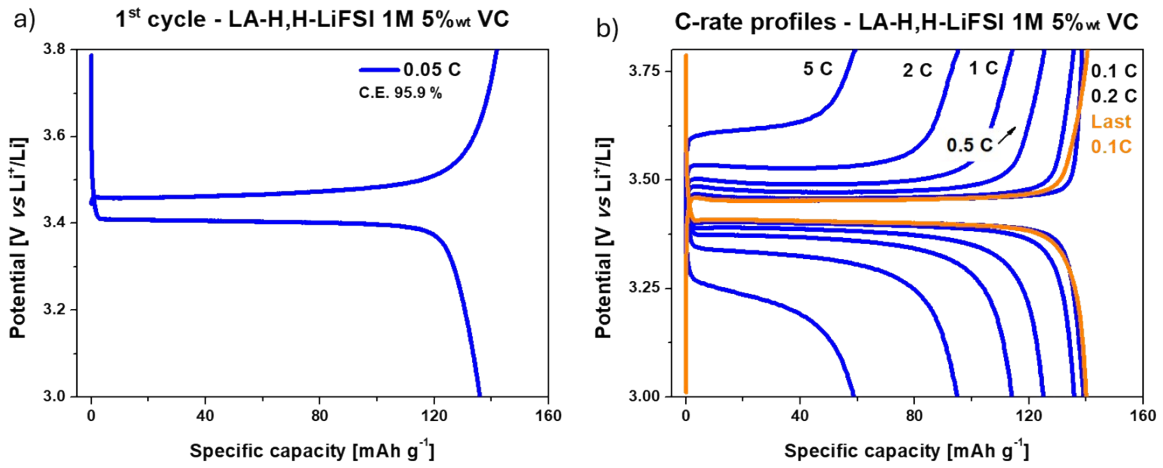


**Fig. S7.** LFP galvanostatic charge/discharge profile with LA-H,H-LiFSI 1M VC 5%<sub>wt</sub> of a) 1<sup>st</sup> cycle at 0.05 C, and b) profiles at different current densities over capability test. C.E.: Coulombic Efficiency.

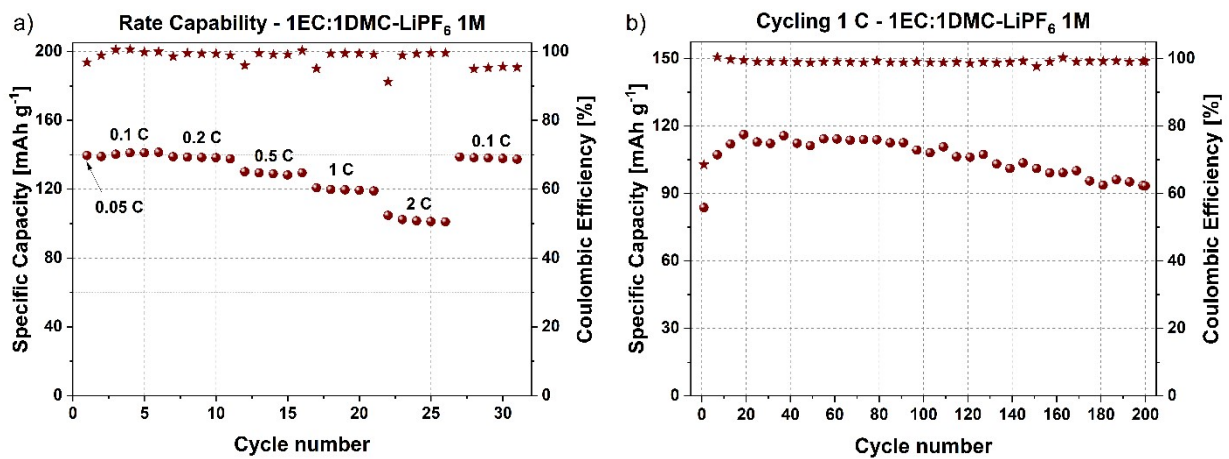


**Fig. S8.** a) Rate capability and b) cyclability of 1EC:1DMC-LiPF<sub>6</sub> 1M electrolyte (LP30) with LFP electrodes.

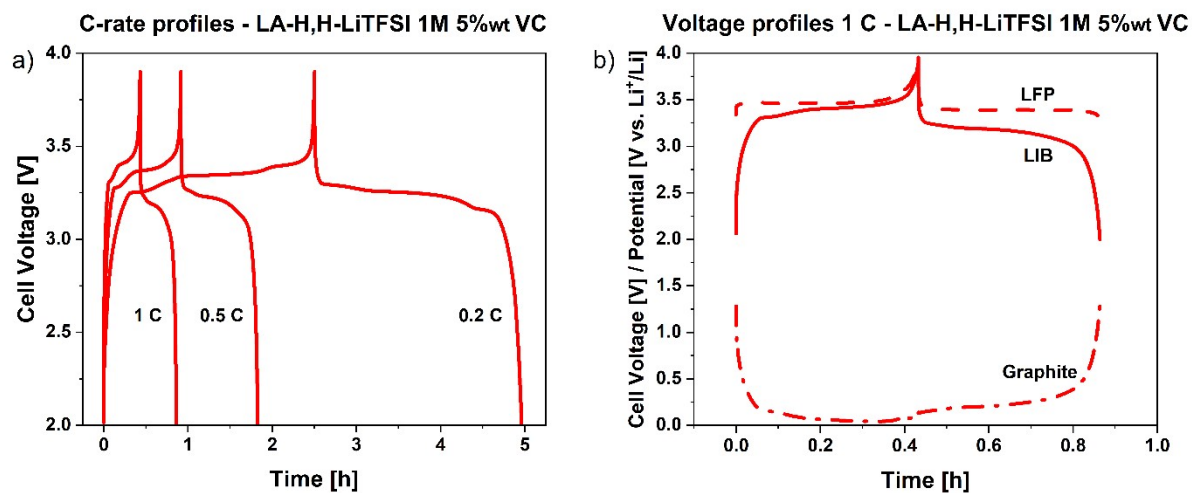


**Fig. S9.** LFP/graphite LIB full-cell a) galvanostatic charge/discharge profiles with LA-H,H-LiTFSI 1M VC 5%wt for noted current densities, and b) profiles of the full-cell, LFP and graphite electrode at 1 C.



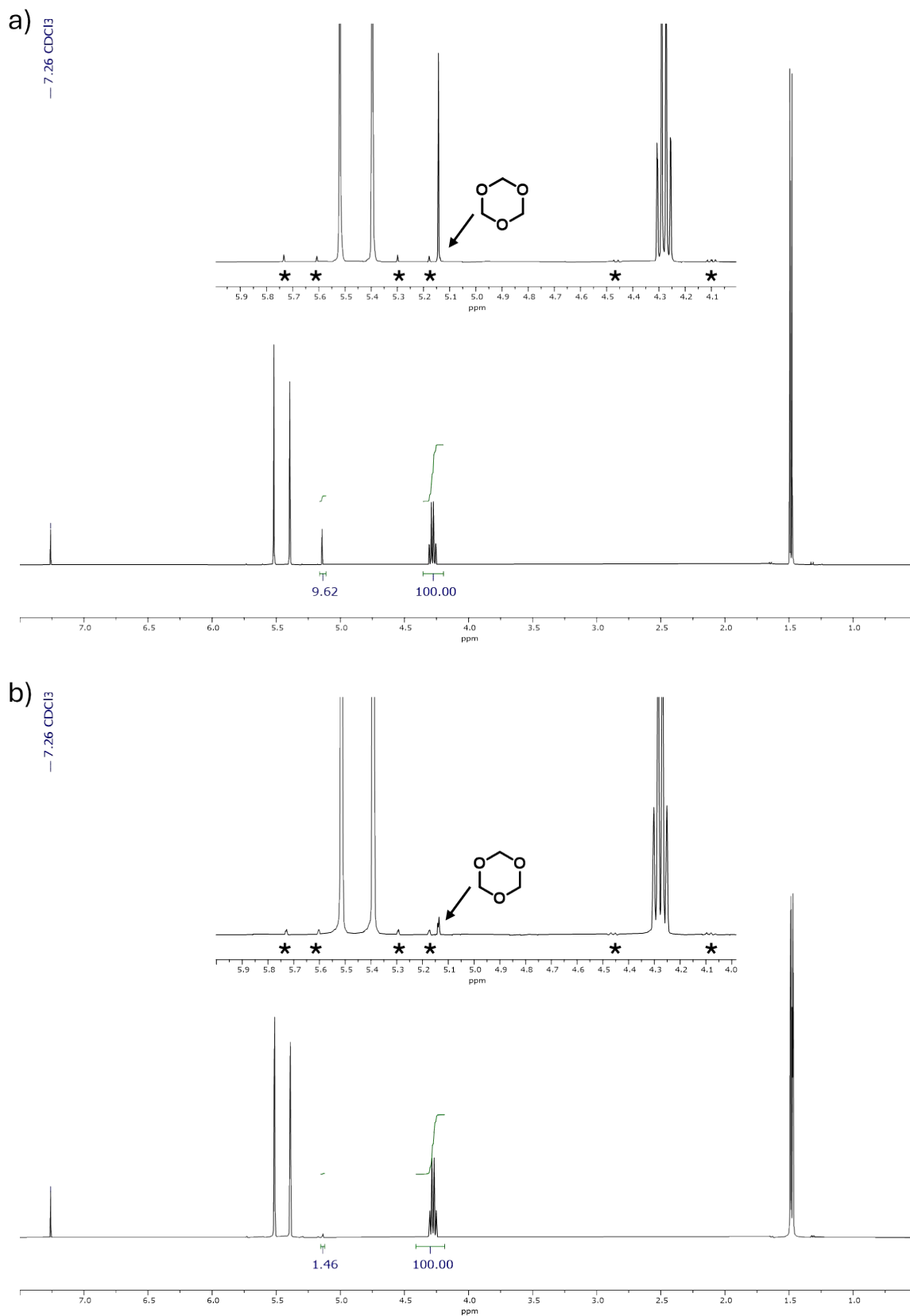


**Fig. S10.** Relevant <sup>1</sup>H NMR spectra (80-100 mg in 0.5 mL CDCl<sub>3</sub>) of LA-H,H distillation: a) “head”, and b) core fractions. Asterisks (\*) are used to highlight <sup>13</sup>C coupling. LA-H,H purity is evaluated by the ratio of the normalized integrals. In spectrum a) the purity was assessed < 99 % (98.4 %), while in spectrum b) it was assessed > 99 % (99.7 %).

### Paragraph S1. NMR analysis details.

Solvent batches with impurities > 1% have been discarded or redistilled until > 99 % is achieved. Typically, discarding the first distillation portion (3-5 mL) from the head fraction is enough to ensure the target purity in the core fraction. The main impurity found during the investigation was identified as trioxane at 5.13-5.14 ppm. Other identified side products from the crude reaction mixture are lactate oligomers, which remain in the distillation tail, and paraformaldehyde oligomers residues, which degrade during the vacuum-distillation process. Formaldehyde contaminants, if present, can be found at 9.7 ppm, and at 4.7-4.6 ppm in its hydrated form (e.g.  $(\text{HO}(\text{CH}_2\text{O})_2\text{H})$  and  $(\text{CH}_2(\text{OH})_2)$ )<sup>15</sup>.

### References

1. Ethylene carbonate, <https://www.sigmaaldrich.com/IT/it/product/mm/844011>, (accessed 07 December, 2024).
2. Dimethyl carbonate, <https://www.sigmaaldrich.com/IT/it/product/sial/517127> (accessed 7 December, 2024).
3. F. A. Kreth, L. Köps, C. Leibing, S. Darlami Magar, M. Hermesdorf, K. Schütjajew, C. Neumann, D. Leistenschneider, A. Turchanin and M. Oschatz, *Advanced Energy Materials*, 2024, **14**, 2303909.
4. L. B. Silva and L. C. G. Freitas, *Journal of Molecular Structure: THEOCHEM*, 2007, **806**, 23-34.
5. J. Wisniak, G. Cortez, R. D. Peralta, R. Infante, L. E. Elizalde, T. A. Amaro, O. García and H. Soto, *The Journal of Chemical Thermodynamics*, 2008, **40**, 1671-1683.
6. K. Kanayama, S. Takahashi, H. Nakamura, T. Tezuka and K. Maruta, *Combustion and Flame*, 2022, **245**, 112359.
7. A. Rodríguez, J. Canosa, A. Domínguez and J. Tojo, *Journal of Chemical & Engineering Data*, 2003, **48**, 146-151.
8. A. Hofmann, M. Migeot, E. Thißen, M. Schulz, R. Heinzmann, S. Indris, T. Bergfeldt, B. Lei, C. Ziebert and T. Hanemann, *ChemSusChem*, 2015, **8**, 1892-1900.
9. CSID:13888876, 5-methyl-1,3-dioxolan-4-one, <https://www.chemspider.com/Chemical-Structure.13888876.html>, (accessed 7 December, 2024).
10. M. Melchiorre, P. H. M. Budzelaar, M. E. Cucciolo, R. Esposito, E. Santagata and F. Ruffo, *Green Chemistry*, 2023, **25**, 2790-2799.
11. M. Ding, K. Xu and T. Jow, *Journal of thermal analysis and calorimetry*, 2000, **62**, 177-186.
12. A. Ponrouch, E. Marchante, M. Courty, J.-M. Tarascon and M. R. Palacín, *Energy & Environmental Science*, 2012, **5**, 8572-8583.
13. N. Yao, X. Chen, X. Shen, R. Zhang, Z. H. Fu, X. X. Ma, X. Q. Zhang, B. Q. Li and Q. Zhang, *Angewandte Chemie*, 2021, **133**, 21643-21648.
14. European Chemical Agency (ECHA), <https://echa.europa.eu/substance-information/>, (accessed 27 November, 2024).
15. M. Rivlin, U. Eliav and G. Navon, *The Journal of Physical Chemistry B*, 2015, **119**, 4479-4487.